GEOPHYSICAL RESEARCH LETTERS, VOL. 39, L14201, doi:10.1029/2012GL052119, 2012

An upper limit for ice in Shackleton crater as revealed by LRO Mini-RF orbital radar

B. J. Thomson,[1] D. B. J. Bussey,[2] C. D. Neish,[2] J. T. S. Cahill,[2] E. Heggy,[3] R. L. Kirk,[4] G. W. Patterson,[2] R. K. Raney,[2] P. D. Spudis,[5] T. W. Thompson,[3] and E. A. Ustinov[3]

Received 23 April 2012; revised 15 June 2012; accepted 16 June 2012; published 28 July 2012.

[1] Although diverse measurements have indicated H^+, OH^-, or H_2O species in the lunar polar regions, pinpointing its location, form, and abundance in specific reservoirs has proven elusive. Here we report on the first orbital radar measurements of Shackleton crater near the lunar south pole. Mini-RF observations indicate a patchy, heterogeneous enhancement in CPR (circular polarization ratio) on the crater walls whose strength decreases with depth toward the crater floor, a result that is most consistent with a roughness effect due to less mature regolith present on the crater wall slopes. However, the results do not rule out a modest ice contribution, and an upper limit of ∼5–10 wt% H_2O ice (up to 30 vol.%) present in the uppermost meter of regolith is also consistent with the observations. **Citation:** Thomson, B. J., et al. (2012), An upper limit for ice in Shackleton crater as revealed by LRO Mini-RF orbital radar, *Geophys. Res. Lett.*, *39*, L14201, doi:10.1029/2012GL052119.

1. Introduction

[2] It has long been recognized that areas of permanent shadow inside polar impact craters are potential sites of volatile accumulation [*Urey*, 1952; *Watson et al.*, 1961; *Arnold*, 1979] due to the Moon's low orbital inclination (∼1.6°) with respect to the ecliptic plane. Orbital neutron measurements indicate elevated levels of near-surface hydrogen (allotropic form undetermined) in the polar regions [*Feldman et al.*, 1998; *Elphic et al.*, 2007; *Mitrofanov et al.*, 2010]; if in the form of water, it would represent an average ice concentration of 1.5 ± 0.8 wt.% in the upper meter of regolith [*Feldman et al.*, 2001]. Near-infrared spectral measurements reveal a hydration signature attributable to OH/H_2O species whose strength increases poleward [*Pieters et al.*, 2009]. Furthermore, the recent LCROSS spacecraft's controlled collision with a permanently shadowed polar region near the lunar south pole revealed evidence for water in its ejecta at an abundance level of a few percent [*Colaprete et al.*, 2010]; mass spectrometer measurements made during descent of the Moon Impact Probe on Chandrayaan-1 also suggest active volatile transport processes [*Sridharan et al.*, 2010].

[3] Radar is an optimal instrument for detecting thick deposits of water-ice for three reasons. First, unlike passive measurement techniques, which rely on the Sun as a source of illumination, radar can illuminate shadowed regions. Second, thick deposits of water ice have a distinctive radar polarization signature compared to the surrounding silicate regolith, thus enabling its detection [*Ostro*, 1993]. Third, radar can measure volatiles buried beneath the surface, as radar typically penetrates 10 to 20 wavelengths below the surface of highland terrain [*Carrier et al.*, 1991] and likely deeper in ice deposits. However, previous radar measurements of the lunar poles have yielded mixed results.

[4] An impromptu bistatic experiment using the Clementine spacecraft indicated a polarization signature suggestive of ice over Shackleton crater near the south pole [*Nozette et al.*, 1996]. However, detailed follow-up investigations with high resolution, Earth-based radar revealed evidence for high CPR (circular polarization ratio) values present high on Shackleton's walls, suggesting a source other than accumulations of slab-like ice [*Campbell et al.*, 2003, 2006]. The maximum albedo of the crater floor as measured by scattered sunlight is also inconsistent with abundant surficial ice [*Haruyama et al.*, 2008].

[5] Here we report on new orbital radar measurements of the crater Shackleton (20 km diameter, centered at 89.63°S, 132.32°E) using the Mini-RF instrument on the Lunar Reconnaissance Orbiter (LRO) spacecraft. We use these measurements to constrain some of the physical properties of the integrated volume of regolith sampled by radar inside Shackleton.

2. Methodology

[6] Mini-RF is a dual-band, synthetic aperture radar (SAR) onboard LRO [*Raney*, 2007; *Nozette et al.*, 2010; *Raney et al.*, 2011] operating in the S-band (2.38 GHz, 12.6 cm wavelength) or X-band (7.14 GHz, 4.2 cm wavelength). Here we concentrate on the S-band data acquired in zoom mode (15 × 30 m spatial resolution). Inherent in the oblique viewing geometry of a SAR instrument is a parallax distortion introduced by terrain height variations. This topography-induced distortion causes points above the surrounding surface to be displaced in the near-range direction of the sensor, and low topographic points are displaced away from the near range. Using a 256 ppd gridded topographic dataset from the Lunar Orbiter Laser Altimeter (LOLA) instrument [*Smith et al.*, 2010], we have corrected for this effect on a pixel-by-pixel basis in a procedure akin to orthorectifying an aerial photograph. To place an upper

[1]Center for Remote Sensing, Boston University, Boston, Massachusetts, USA.
[2]Johns Hopkins University Applied Physics Laboratory, Laurel, Maryland, USA.
[3]Jet Propulsion Laboratory, Pasadena, California, USA.
[4]U.S. Geological Survey, Flagstaff, Arizona, USA.
[5]Lunar and Planetary Institute, Houston, Texas, USA.

Corresponding author: B. J. Thomson, Center for Remote Sensing, Boston University, 725 Commonwealth Ave., Room 433, Boston, MA 02155, USA. (bjt@bu.edu)

0094-8276/12/2012GL052119

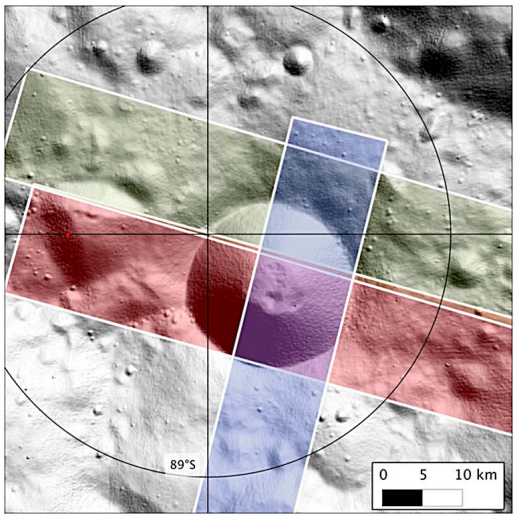

Figure 1. LOLA 256 ppd topographic shaded relief map of lunar south polar region. The position of Mini-RF observations of Shackleton Crater are indicated by the colored boxes (red = 2010-04-18 observation; yellow = 2010-06-25 observation; blue = 2009-12-23 observation).

constraint on the amount of water-ice present in the near surface, we used a semi-empirical model of a silicate-ice mixture to create synthetic SAR images containing a set percentage of ice, present as decimeter-sized or larger blocks [*Lichtenberg*, 2000], and compared them to the topographically corrected Mini-RF swaths. The model utilizes a combination of a theoretical model of the coherent backscatter opposition effect [*Mishchenko*, 1992] and ground-based radar data of the Moon [*Evans et al.*, 1968]; additional details are given in the Text S1 and Figure S1 in the auxiliary material.[1]

3. Shackleton Crater Observations

[7] Three separate observations of Shackleton Crater were made on 23 Dec. 2009, 18 Apr. 2010, and 26 Jun 2010 (Figure 1). Due to the proximity of Shackleton to the lunar south pole, the LRO spacecraft had to roll 14–19° toward the nadir position to bring the crater into the radar field of view. This resulted in angles of incidence ranging from 28–32° compared to the nominal Mini-RF incidence of about 48°. A comparison of the synthetic SAR model output with the actual data is given in Figures 2a–2c. In Figure 2a, data from 18-Apr-2010 is compared with modeled ice contents that range from 0 to 10 wt%. Enhanced CPR values are restricted to the interior of the crater only, and although the distribution is patchy, the results are consistent with a modeled ice content ~5–10 wt% H_2O. Regions within the crater are also consistent with a modeled ice content ~5 wt% in Mini-RF data from 2009-12-23 (Figure 2b). However, some enhanced CPR values are observed outside the crater rim in this image (elevated CPR also arises naturally from rough, rock-rich proximal impact ejecta). In the third observation of Shackleton crater (Figure 2c), the observation geometry was not particularly favorable to exhibit CPR enhancements due

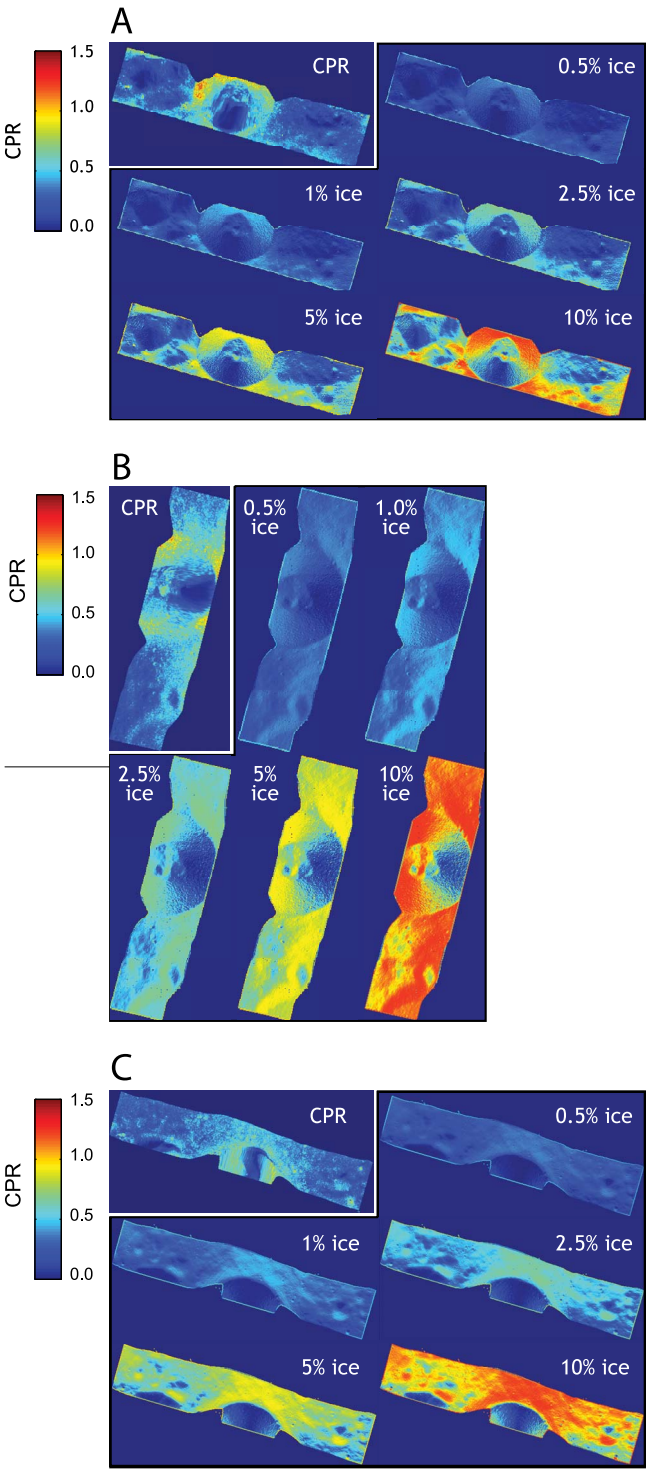

Figure 2. (a) Mini-RF data from 2010-04-18 of Shackleton (Mini-RF swath LSZ_03737_2CD_OKU_90S137_V1). Upper left panel is measured CPR data; other panels show synthetic CPR values calculated using a semi-empirical model of an ice-silicate mixture. Ice contents of 0.5, 1.0, 2.5, 5, and 10 wt% H_2O ice are given. (b) Same as Figure 2a with Shackleton data from 2009-12-23 (Mini-RF swath LSZ_02261_2CD_OKU_89S140_V1). (c) Same as Figures 2a and 2b with Shackleton data from 2010-06-25 (Mini-RF swath LSZ_04605_2CD_OKU_90S061_V1).

[1]Auxiliary materials are available in the HTML. doi:10.1029/2012GL052119.

to water-ice, regardless of the exact amount at which might be present. A small region of enhanced CPR in visible in the crater interior, consistent with a modeled ice content of perhaps 5–10 wt% H_2O-ice. As with the 2009-12-23 data, a slight CPR enhancement is discernable outside the crater's rim. Apart from differences due to variations local slope, measured CPR values are fairly consistent in different radar observations (e.g., flat areas outside the craters visible in multiple swaths).

4. Discussion

[8] Although the models indicate that the crater walls are plausibly consistent with a small amount of ice, the crater floor exhibits little to no enhancement (see Figure 2a). Indeed, CPR values tend to decrease with depth into the crater (Figure S2). Furthermore, if high CPR values within Shackleton are due to volume scattering within ice, one would expect to see a discontinuity or jump in CPR values on the crater wall that marks the transition from seasonally sunlit to permanently shadowed regions [*Campbell et al.*, 2006]. Although the occurrences of high CPR areas on the crater walls are patchy, no specific discontinuities are evident. The totality of these characteristics is consistent with the downslope movement of material causing higher than average decimeter-scale surface roughness on the crater walls than is present in the average mature regolith that develops on flatter surfaces. Although these observations are suggestive of the fact that the CPR signature is dominantly due to a factor unaffected by the presence or absence of sunlight (i.e., mass wasting), a component due a modest abundance of ice cannot be ruled out. If, for example, the kinetics of volatile migration in partially sunlit surfaces adjacent to regions of permanent shadow is such that the volatile replenishment process is rapid or the removal processes is slow, some volatiles may be retained. Modeling results of ice diffusion in regolith suggest that diurnal temperature oscillations, such as those typical of permanently shaded regions adjacent to occasionally sunlit areas, can actually enhance the accumulation of ice within the uppermost meter of the surface [*Schorghofer and Taylor*, 2007]. In either case, the Mini-RF measurements place an upper bound on the ice content of the uppermost meter of regolith with Shackleton of ~5–10 wt% H_2O ice. This finding is consistent with slight albedo enhancements observed in Shackleton at optical wavelengths (430–850 nm) as measured with scattered light [*Haruyama et al.*, 2008] and at far ultraviolet wavelengths (155–190 nm) as measured by Lyman Alpha Mapping Project (LAMP) [*Gladstone et al.*, 2012], indicating a surface exposure of at most a few percent of high albedo material (e.g., water-ice) mixed with typical highland material. Near-infrared reflectance measurements from LOLA also indicate a slight brightening within Shackleton due to either mass wasting or possibly up to ~20% water ice frost in the uppermost nm [*Zuber et al.*, 2012].

[9] The fundamental conclusions made with high resolution, ground based radar of Shackleton remain unaltered – that no large-scale, meters thick ice deposits are evident within the crater. Rather, Mini-RF data are consistent with roughness effects or with a small percentage of water-ice deposits admixed into the uppermost 1–2 meters of silicate regolith within Shackleton, possibly accounting for the observations made by the Clementine bistatic experiment.

[10] **Acknowledgments.** We thank the LRO project and the Mini-RF engineers and scientists who made the rolled observations, data collection, and data calibration a reality. This research has made use of the USGS Integrated Software for Imagers and Spectrometers (ISIS) software for data processing and MATLAB® software for data analysis. Comments from an anonymous reviewer improved the manuscript.

[11] The Editor thanks the anonymous reviewer for assisting in the evaluation of this paper.

References

Arnold, J. R. (1979), Ice in the lunar polar regions, *J. Geophys. Res.*, *84*, 5659–5668, doi:10.1029/JB084iB10p05659.

Campbell, B. A., D. B. Campbell, J. F. Chandler, A. A. Hine, M. C. Nolan, and P. J. Perillat (2003), Radar imaging of the lunar poles, *Nature*, *426*, 137–138, doi:10.1038/426137a.

Campbell, D. B., B. A. Campbell, L. M. Carter, J.-L. Margot, and N. J. S. Stacy (2006), No evidence for thick deposits of ice at the lunar south pole, *Nature*, *443*, 835–837, doi:10.1038/nature05167.

Carrier, W. D. I., G. R. Olhoeft, and W. Mendell (1991), Physical properties of the lunar surface, in *Lunar Sourcebook*, edited by G. H. Heiken et al., pp. 475–594, Cambridge Univ. Press, Cambridge, U. K.

Colaprete, A., et al. (2010), Detection of water in the LCROSS ejecta plume, *Science*, *330*, 463–468, doi:10.1126/science.1186986.

Elphic, R. C., V. R. Eke, L. F. A. Teodoro, D. J. Lawrence, and D. B. J. Bussey (2007), Models of the distribution and abundance of hydrogen at the lunar south pole, *Geophys. Res. Lett.*, *34*, L13204, doi:10.1029/2007GL029954.

Evans, J. V., T. Hagfors, and G. H. Pettengill (1968), Radar studies of the Moon, final report, 99 pp., Lincoln Lab., Lexington, Mass.

Feldman, W. C., S. Maurice, A. B. Binder, B. L. Barraclough, R. C. Elphic, and D. J. Lawrence (1998), Fluxes of fast and epithermal neutrons from Lunar Prospector: Evidence for water ice at the lunar poles, *Science*, *281*, 1496–1500, doi:10.1126/science.281.5382.1496.

Feldman, W. C., et al. (2001), Evidence for water ice near the lunar poles, *J. Geophys. Res.*, *106*, 23,231–23,251, doi:10.1029/2000JE001444.

Gladstone, G. R., et al. (2012), Far-ultraviolet reflectance properties of the Moon's permanently shadowed regions, *J. Geophys. Res.*, *117*, E00H04, doi:10.1029/2011JE003913.

Haruyama, J., et al. (2008), Lack of exposed ice inside lunar south pole Shackleton Crater, *Science*, *322*, 938, doi:10.1126/science.1164020.

Lichtenberg, C. L. (2000), Bistatic radar observations of the moon using the Clementine spacecraft and Deep Space Network, PhD thesis, 464 pp., Johns Hopkins Univ., Baltimore, Md.

Mishchenko, M. I. (1992), Polarization characteristics of the coherent backscatter opposition effect, *Earth Moon Planets*, *58*, 127–144, doi:10.1007/BF00054650.

Mitrofanov, I. G., et al. (2010), Hydrogen mapping of the lunar south pole using the LRO Neutron Detector Experiment LEND, *Science*, *330*, 483–486, doi:10.1126/science.1185696.

Nozette, S., C. L. Lichtenberg, P. Spudis, R. Bonner, and W. Ort (1996), The Clementine bistatic radar experiment, *Science*, *274*, 1495–1498, doi:10.1126/science.274.5292.1495.

Nozette, S., et al. (2010), The Lunar Reconnaissance Orbiter Miniature Radio Frequency (Mini-RF) technology demonstration, *Space Sci. Rev.*, *150*, 285–302, doi:10.1007/s11214-009-9607-5.

Ostro, S. J. (1993), Planetary radar astronomy, *Rev. Mod. Phys.*, *65*(4), 1235–1279, doi:10.1103/RevModPhys.65.1235.

Pieters, C. M., et al. (2009), Character and spatial distribution of OH/H_2O on the surface of the Moon seen by M^3 on Chandrayaan-1, *Science*, *326*, 568–572, doi:10.1126/science.1178658.

Raney, R. K. (2007), Hybrid-polarity SAR architecture, *IEEE Trans. Geosci. Remote Sens.*, *45*(11), 3397–3404, doi:10.1109/TGRS.2007.895883.

Raney, R. K., et al. (2011), The lunar Mini-RF Radars: Hybrid polarimetric architecture and initial results, *Proc. IEEE*, *99*(5), 808–823, doi:10.1109/JPROC.2010.2084970.

Schorghofer, N., and G. J. Taylor (2007), Subsurface migration of H_2O at lunar cold traps, *J. Geophys. Res.*, *112*, E02010, doi:10.1029/2006JE002779.

Smith, D. E., et al. (2010), Initial observations from the Lunar Orbiter Laser Altimeter (LOLA), *Geophys. Res. Lett.*, *37*, L18204, doi:10.1029/2010GL043751.

Sridharan, R., S. M. Ahmed, T. Pratim Das, P. Sreelatha, P. Pradeepkumar, N. Naik, and G. Supriya (2010), The sunlit lunar atmosphere: A comprehensive study by CHACE on the Moon Impact Probe of

Chandrayaan-1, *Planet. Space Sci.*, *58*, 1567–1577, doi:10.1016/j.pss.2010.07.027.

Urey, H. C. (1952), *The Planets: Their Origin and Development*, 245 pp., Yale Univ. Press, New Haven, Conn.

Watson, K., B. Murray, and H. Brown (1961), On the possible presence of ice on the Moon, *J. Geophys. Res.*, *66*, 1598–1600, doi:10.1029/JZ066i005p01598.

Zuber, M. T., et al. (2012), Constraints on the volatile distribution within Shackleton crater at the lunar south pole, *Nature*, *786*, 378–381, doi:10.1038/nature11216.